ON THE NUMERICAL CALCULATION OF IMPINGING JETS

Bruno R. G. da Silva
Mechanical Engineering Department (DEM/EE/UFRJ),
C.P. 68503, 21945-970 - Rio de Janeiro – Brazil.
brunorgs@yahoo.com.br

Danielle R. S. Guerra
Mechanical Engineering Department (CT/DEM/UFPA)
66090-000, Belém – Pará
daguerra@ufpa.br

Atila P. Silva Freire
Mechanical Engineering Program (PEM/COPPE/UFRJ)
C.P. 68503, 21945-970, Rio de Janeiro, Brazil
atila@mecanica.coppe.ufrj.br

Abstract*. The present work investigates the applicability of various turbulence models for the numerical simulation of a jet impinging orthogonally onto a wall. The following models are tested: the SST κ–ω Model and the BSL Reynolds stress model. The results are compared with data specially devised for the velocity field, turbulence intensity profiles and skin-friction at the wall. Overall, the authors show that the SST model provides the best results. The experiments were conducted for one nozzle-to-plate spacing (H/D = 2.0) and Reynolds number of 35.000. A particular interest of the work is the investigation of the applicability of scaling log-laws to the turbulent impinging jet.*

Keywords. *Turbulence, jet, impingement, scaling laws.*

1. Introduction

Turbulent impinging jets have been a subject of wide interest in the recent times. The reason for this is clear, impinging jets constitute a primary means of cooling hot surfaces. As such, practical applications span a broad range, extending from the cooling of heated components in gas turbine to the cooling of micro-mechanical devices. Other applications include tempering and shaping of glass, the annealing of plastic and metal sheets, the drying of textile and paper products, the deicing of aircraft systems and engines and electronic instruments.

Despite all this recent interest, it is a plain fact that most works published in the literature deal most with the heat transfer process, in prejudice of a hydrodynamics analysis of the problem. This is also very understanding. Typically, the flow region near the stagnation point is very active in terms of the occurring physical processes, but yet very small in size. That single feature makes the business of measuring the flow properties near the stagnation point a very difficult affair. On the other hand, knowledge about the distribution of shear stress around the stagnation point is crucial for a good understanding of the problem. This last remark is particularly aggravated if we consider that many turbulence models rely on simple analogies between the processes of momentum transfer and heat transfer. For the impinging jet, however, we know that at the stagnation point the shear stress is zero but the heat transfer is different from zero. The implication is that, at stagnation, the Reynolds analogy between eddy-diffusivity and eddy-viscosity breaks down.

Still, turbulence models of the eddy viscosity type have been used by some authors together with some heat transfer analogy considerations for the description of the temperature field (see, e.g., Behnia et al. (1998, 1999), Gibson e Harper (1997)) to produce numerical predictions of impinging jets. Lee and Lee (1999, 2000), Kendoush (1998), Nishino et al. (1996)) also investigated the behavior of the heat transfer coefficient at a stagnation point. However, if simple analogies are used, when the equations of motion are integrated to the wall and the hypothesis of a constant turbulent Prandtl number is used, the calculated heat transfer rates at the stagnation point are observed to exceed by much their actual values.

In any case, the performance of turbulent models to predict the behavior of an impinging jet has been examined by many authors. In particular, low Reynolds number kappa-epsilon models, Reynolds stress models, and the kappa-omega model have been tried. This will be shortly reviewed in the next section.

The purpose of the present work is two-fold: i) to perform numerical simulations of an orthogonal jet impinging onto a surface via some alternative turbulent models, in special, a Shear Stress Turbulence Model and a Baseline Reynolds Stress Model and ii) to carry out further investigations on the scaling laws that govern the motion of an impinging jet. For the latter matter, the law of the wall for the velocity field will be investigated in detail. In fact, as we shall see, this is a necessary first step for the investigation of some governing parameters on the skin-friction and on the heat transfer characteristics of a circular impinging jet on a heated flat plate.

The relevance of the present study lies on the fact that the use of wall functions to by-pass the difficulties involved with the modeling of low Reynolds number turbulence is still an attractive means to solve problems in a simple way. For instance, Cruz and Silva Freire (1998, 2002) have proposed an alternative approach where new wall functions are

used to describe the velocity and temperature fields in the wall logarithmic region of a separating flow. As the stagnation point is approached, these functions reduce to power-law solutions recovering Stratford's solution. The papers of Cruz and Silva Freire resorted to Kaplun limits for an asymptotic representation of the velocity and temperature fields. Results were presented for the asymptotic structure of the flow and for the skin-friction coefficient and Stanton number at the wall. An investigation on the wall scaling near stagnation might, then, produce a simple near wall expression that can be used to discriminate the local boundary conditions for the velocity and the temperature fields.

As much as we have some experimental data under our disposal to investigate the flow behavior in the wall region of the flow, it is of utmost importance to detail the flow near a stagnation point. For this reason, the present investigation is set under way: to furnish reliable numerical data for an investigation of any possible existing logarithmic behavior of the velocity profile. In particular, and as mentioned before, two turbulence models were selected the SST model and the BSL Reynolds Stress Model.

2. Numerical methods

2.1 Governing equations

Turbulence is ubiquitous in nature and engineering. However, its inherent features consisting of high frequency fluctuations in time and space make it a formidable problem to deal with.

The Navier-Stokes equations are the governing equations for all types of flow regime, including turbulent flow. However, at realistic Reynolds numbers the length and time scales present in the flow span such a large spectrum that any attempt at resolving the flow down the smallest scales results in a sound physical impossibility due to present computer power. To overcome the difficulties imposed by the richness in relevant scales present in the flow, a current practice is to resort to *turbulence models*.

Turbulence models are obtained by modifying the Navier-Stokes equations to introduce averaged and fluctuating quantities. Then, the continuity and the two-dimensional, incompressible Reynolds averaged Navier-Stokes equations reduce to

$$\frac{\partial \overline{u_i}}{\partial x_i} = 0 \tag{1}$$

$$\frac{\partial \overline{u_i}}{\partial t} + u_i \frac{\partial \overline{u}_j}{\partial x_i} = -\frac{1}{\rho}\frac{\partial \overline{p}}{\partial x_i} + \frac{\partial}{\partial x_j}\left(\upsilon \frac{\partial \overline{u_i}}{\partial x_j} + \frac{\partial \overline{u_j}}{\partial x_i} \right) - \frac{\partial}{\partial x_j}\left(\overline{u'_i u'_j}\right) \tag{2}$$

where capital letters are used for the time-averaged quantities and small letters to the fluctuating quantities. The notation is classical. Thus, $u'_i u'_j$ denotes the Reynolds stress.

Turbulence models provide mathematical models for the Reynolds stress. In general compendia in fluid mechanics, these models are basically divided into two classes: eddy viscosity models and Reynolds stress models. In the present work, two turbulence models were chosen for scrutiny, one from each different classification: an eddy viscosity models, the SST κ–ω Based Model and a Reynolds stress model, the BSL RSM. These will be discussed next.

2.2 The SST κ–ω model

Eddy viscosity turbulence models consider that the Reynolds stress can be related to the mean velocity gradients through the rate of strain tensor and an eddy viscosity, so that one can write

$$-\overline{u'_i u'_j} = \nu_t \left(\frac{\partial \overline{u_i}}{\partial x_j} + \frac{\partial \overline{u_j}}{\partial x_i} \right) - \frac{2}{3}\kappa \delta_{ij} \tag{3}$$

where ν_t denotes the eddy viscosity and δ_{ij} is the Kronecker delta.

In two-equation models, the turbulent viscosity is specified through two transportable characteristic quantities of the flow. These quantities are then to be found from differential equations that must be derived directly from the Reynolds equations. Typical transportable quantities used to specify the turbulent viscosity are the turbulent kinetic energy, κ, the dissipation per unit mass, ε, and, the specific dissipation rate, ω.

The κ–ω model considers that the turbulent viscosity is relater to the turbulent kinetic energy and the turbulent frequency through expression

$$\mu_\tau = \rho\ (\kappa/\omega) \tag{4}$$

The κ–ω formulation has become very popular over the last few years for its apparent superior performance for the treatment of near wall conditions. The κ–ω model does not require the introduction of the typical non-linear dumping functions present in the κ–ε model and, for this reason, should be more accurate and robust. As a matter of fact, the κ–ω model can be resolved with a near wall resolution of y+ < 2.

The two transport equations for the κ–ω model can be written as

$$\frac{\partial \kappa}{\partial t} + \overline{u_i} \frac{\partial \kappa}{\partial x_i} = \frac{\partial}{\partial x_i}\left[\left(\upsilon + \left(\frac{\upsilon_t}{\sigma_\kappa}\right)\right)\frac{\partial \kappa}{\partial x_i}\right] + P_k - \beta' \kappa\omega \tag{5}$$

$$\frac{\partial \omega}{\partial t} + \overline{u_i} \frac{\partial \omega}{\partial x_i} = \frac{\partial}{\partial x_i}\left[\left(\upsilon + \left(\frac{\upsilon_t}{\sigma_\omega}\right)\right)\frac{\partial \omega}{\partial x_i}\right] + \alpha \frac{\omega}{k} P_k - \beta\omega^2 \tag{6}$$

$$P_k = -\overline{u_i' u_j'} \frac{\partial \overline{u_j}}{\partial x_i} \tag{7}$$

The κ–ω model constants are given by:

$$\alpha = 5/9$$

$$\beta = 0.075 \qquad \beta' = 0.09$$

$$\sigma_{\kappa 2} = 2 \qquad \sigma_{\omega 2} = 2$$

The Shear Stress Transport (SST) κ–ω Model, accounts for turbulent shear stress transport by considering

$$\upsilon_\tau = \frac{\alpha_1 \kappa}{max(\alpha_1 \omega, SF_2)} \tag{8}$$

where F_2 is a blending function, and S is an invariant measure of the strain rate.

The blending function F_2 is given by

$$F_2 = tanh(arg_2^2) \tag{9}$$

with

$$arg_2 = max\left(\frac{2\sqrt{k}}{\beta' \omega y}, \frac{500\upsilon}{y^2 \omega}\right) \tag{10}$$

2.3 The BSL Reynolds Stress Model

Reynolds Stress Turbulence Models do not use the eddy viscosity hypothesis. Alternatively, the RSM transport equations are solved for each of the six individual stress components.

The Reynolds stress transport equation for ω based models is given by

$$\frac{\partial \tau_{ij}}{\partial t} + \frac{\partial \overline{u}_k \tau_{ij}}{\partial x_k} = P_{ij} + \frac{2}{3}\beta' \omega \kappa \delta_{ij} - P_{ij} + \frac{\partial}{\partial x_k}\left(\left(\upsilon + \frac{\upsilon_t}{\sigma^*}\right)\frac{\partial \tau_{ij}}{\partial x_k}\right) \tag{11}$$

The following coefficients apply:

$$\sigma^* = 2$$

$$\beta = 0.075$$

$$k = 0.41$$

$$\alpha = \frac{\beta}{\beta'} - \frac{k^2}{\sigma(\beta')^{0.5}} = 5/9$$

where the equation for ω is given by

$$\frac{\partial \omega}{\partial t} + \frac{\partial \overline{u}_k \omega}{\partial x_k} = \alpha_3 \frac{\omega}{\kappa} P_\kappa - \beta_3 \omega^2 + \frac{\partial}{\partial x_k}\left(\left(\upsilon + \frac{\upsilon_t}{\sigma_{\omega 3}}\right)\frac{\partial \omega}{\partial x_k}\right) + (1 - F_1) 2 \frac{1}{\sigma_2 \omega} \frac{\partial \kappa}{\partial x_k} \frac{\partial \omega}{\partial x_k} \tag{12}$$

In the above equation, the BSL blending principle is applied so that the coefficients α and β of the ω-equation are obtained from two distinct sets of constants.

For the ω-discriminated region, the corresponding constants are:

$\alpha_3 =$, $\beta_3 =$, $\sigma_{\omega 3} =$, $\sigma_2 =$

For the ε-discriminated region, the corresponding constants are:

$\alpha_3 =$, $\beta_3 =$, $\sigma_{\omega 3} =$, $\sigma_2 =$

Finally, the blending coefficients are found from a linear interpolation through the relation

$$\phi_3 = F\,\phi_1 + (1\text{-}F)\,\phi_2 \tag{13}$$

where

$$F = \tanh(arg^4) \tag{14}$$

with

$$arg = \min\left(\max\left(\frac{\sqrt{k}}{\beta'\omega y}, \frac{500\upsilon}{y^2\omega}\right), \frac{4\rho\kappa}{CD_{\kappa\omega}\sigma_{k-\varepsilon}y^2}\right) \tag{15}$$

and

$$CD_{\kappa\omega} = \max\left(2\rho\frac{1}{\sigma_{\kappa-\varepsilon}\omega}\frac{\partial\kappa}{\partial x_j}\frac{\partial\omega}{\partial x_j}, 10^{-10}\right) \tag{16}$$

3. Experimental setup

The experiments to be introduced here are part of a comprehensive study that has been undertaken by the authors in the last five years. Complementary references to the presence are Guerra and Silva Freire (2003, 2004) and Guerra et al. (2005).

A schematic diagram of the experimental apparatus and the problem geometry can be found in Guerra et al. (2005). For this reason, here, and just for the records, we will make just a few comments on the experimental procedure, which are basically the comments issued in that reference.

Air at 18.5 ^{o}C was pumped through a centrifugal blower and passed through a 1350 mm long pipe with 43.5 mm internal diameter. Inside the pipe, a flow straighten honeycomb was fitted constructed from drinking straws glued together; screens were also set in place. The jet was set to emerge from the circular nozzle with a bulk velocity of 12 m/s.

The distance from the jet nozzle to the wall was 87 mm. This defines a nozzle-to-plate spacing H/D = 2.0.

The impingement flat plate was made of a 3.7 mm thick aluminum circular sheet. This sheet had 840 mm in diameter and was laid over a plenum chamber as shown. The plenum chamber was 20 mm height and 815 mm in diameter. The walls of the plenum were completely insulated from the ambient.

The controlled parameters in the experiments were the nozzle-to-plate spacing and the stagnation pressure. At each test, the centerline of the jet was lined up with the center of the impingement surface.

The temperature of the aluminum sheet was monitored through thermocouples. The readings of the thermocouples were routed to a AMD Athlon +2000 MHz personal computer via a Picolog acquisition system model TC-08.

The jet exit velocity was measured using a Pitot tube and an electronic manometer. Temperature profiles were measured using a chromel-constantan micro-thermocouple that was positioned using a traverse gear system with a sensitivity of 0.02 mm.

The geometrical center of the impingement plate was determined as follows. First, the plate was fitted with 27 pressure taps arranged at a cross formation. The readings of the pressure at these points were then used to find the geometrical center of the jet; only when the pressure distribution was found to be completely symmetric the jet centerline was considered determined.

4. Numerical simulation

All simulations were performed in cylindrical coordinates with the commercial code CFX. The grid was non-uniform, orthogonal, with a near wall high resolution. The size of the meshes varied from 330.000 to 650.000 nodes. A mesh sensitivity study was carried out by doubling the number of the mesh points in both the azimuthal and the radial

directions. Even for the coarser grid, care was taken so as to keep at least 10 point in the viscous region, defined by y+ = 10.9. For most of the flow stations, but for station r = 150 mm, the changes in velocity were within 1%. Figures 1 and 2 illustrate the mesh sensitivity study.

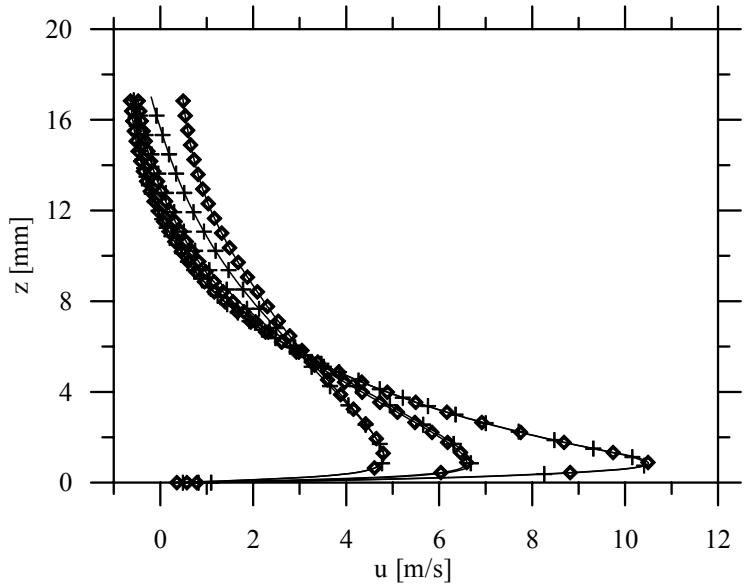

Figure 1. Mesh sensitivity for SST Model. Crosses denote meshes with 330.000 points. Diamonds denote meshes with 650.000 points

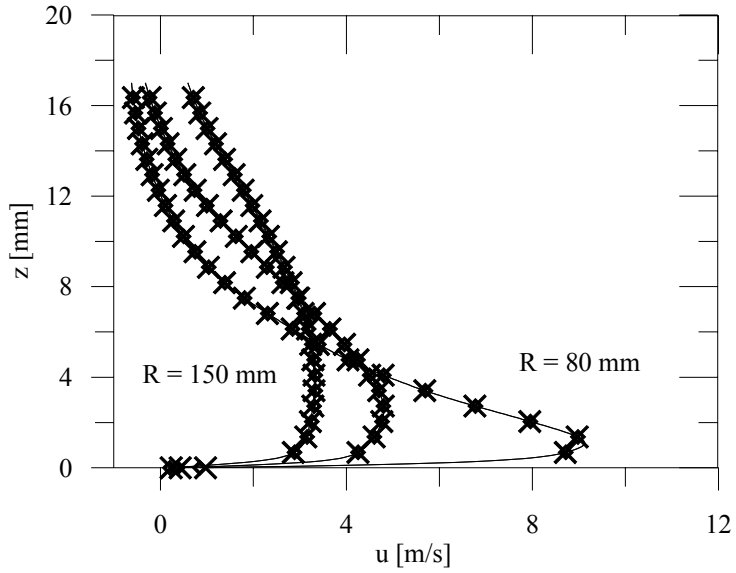

Figure 2. Mesh sensitivity for BSL RSM. Crosses denote meshes with 330.000 points. Diamonds denote meshes with 650.000 points

So that the computed flow field did not suffer from uncertainties in the nozzle conditions, the inlet profiles at the nozzle exit were taken directly from the experiments.

5. Results

The work will present complete results for the geometry defined by the aspect ratio H/D = 2.0.

Predictions on the radial pressure distributions on the impingement surface are shown in Fig. 3. The pressure measurements were non-dimensionalized with the dynamic pressure, $\rho U^2/2$, where ρ is the density of air and U is the jet exit velocity.

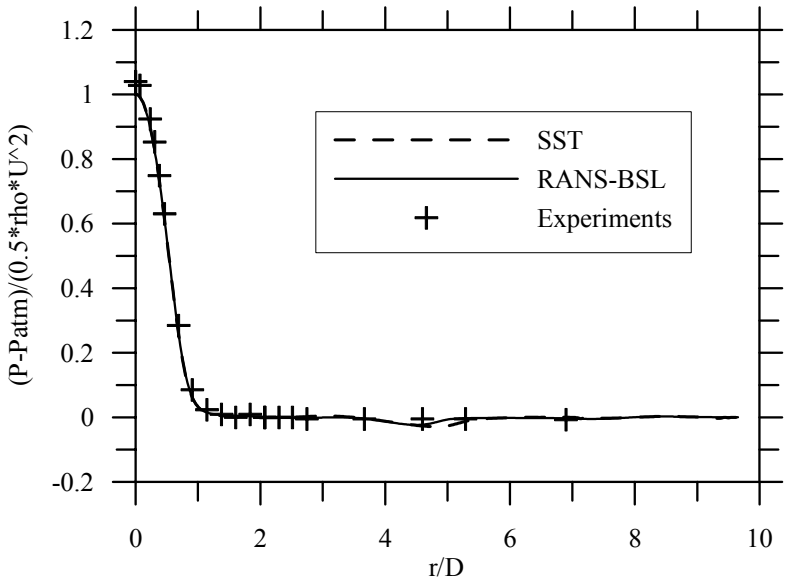

Figure 3. Radial pressure distributions of the jet

To characterize the jet wall spreading, the radial component of the mean velocity was examined at various radial positions.

Numerical predictions of the velocity and turbulent intensity profiles are shown in Figures 4 and 5 compared with the experimental data. Please note that these graphs are presented in linear, dimensional coordinates.

In Gerra et al. (2005), the authors show that, much in the same trend as noticed by Özdemir and Whitelaw (1992, the wall layer solution can be represented by a logarithmic expression provided parameter A in the law of the wall is scaled by the local miaxumun velocity and the skin-friciton velocity. That is, Guerra et al. (2005) showed that, for the near wall region, a semi-log relation can be used to model the inner equilibrium layer.

Thus, it follows that

$$\frac{u}{u_\tau} = \frac{1}{\kappa}\ln\left(\frac{yu_\tau}{\nu}\right) + A \tag{4}$$

$$A = 1.124\left(\frac{u_M}{u_\tau}\right) - 27.538, \tag{5}$$

where κ(=0.4) is the von Karman constant, u_τ is the friction velocity and u_M is the maximum jet velocity at a given station.

The conclusion of Guerra et al. (2995), therefore, was that parameter *A* is not invariant but changes with a deviation function. To describe *A*, these authors proposed a simple relation with the form of Eq. (5).

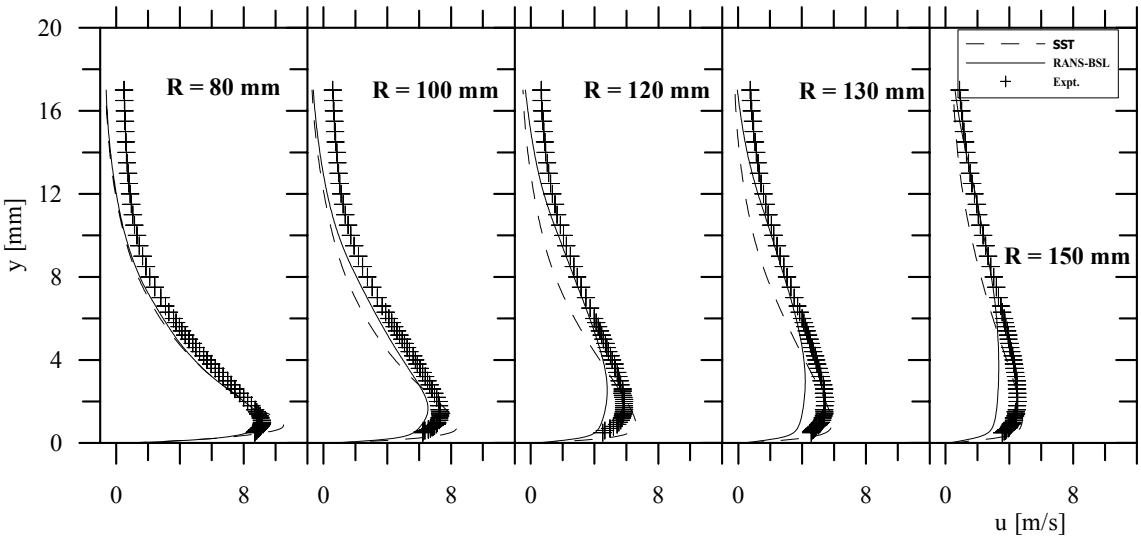

Figure 4. Mean velocity profiles in dimensional variables. Y is given in millimeters.

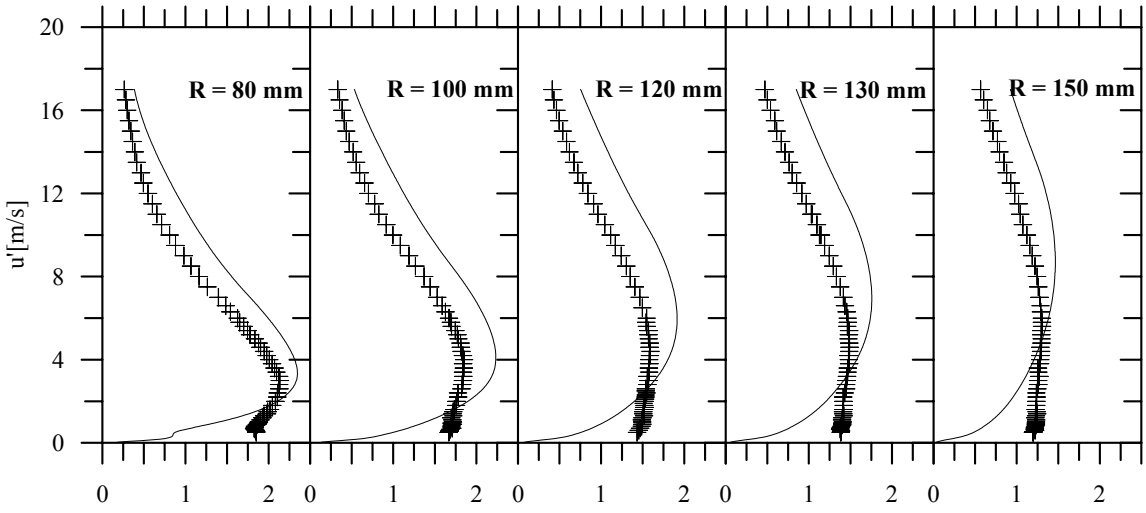

Figure 5. Longitudinal turbulent intensity profiles in dimensional variables.

The implications of the law of the wall are clear. It can be used to serve as wall boundary condition in simulations of the flow that resort to wall law formulations. In addition, it can be used to find the skin-friction velocity provided the point where the maximum longitudinal velocity occurs is known.

Equations 4 and 5 are tested in Figs. 6 and 7.

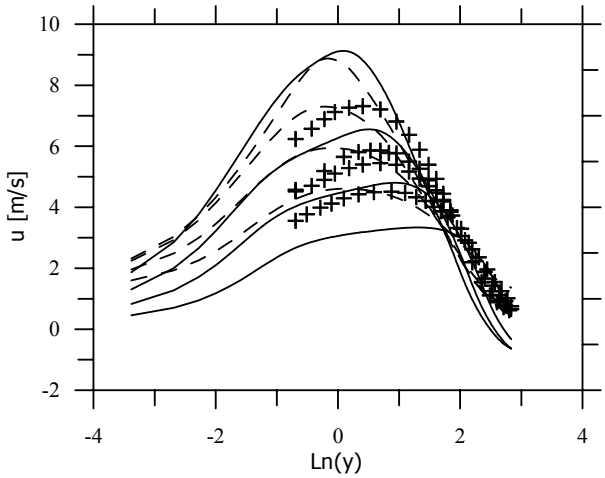

Figure 6. Mean velocity profiles in dimensional variables. Y is given in millimeters.

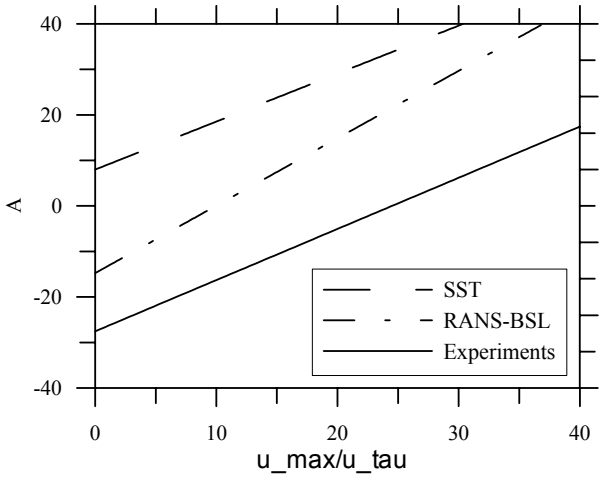

Figure 7. Deviation function for the velocity profiles.

Figure 6 shows the predicted velocity profiles in wall coordinates for several *r*-wise stations. The resulting values of A are shown in Fig. 7.

The predicted values of wall shear stress are presented in Fig. 8.

This figure confirms that *A* increases as the maximum jet velocity increases respectively. Despite the scatter in the data these trends seem to be well defined.

Thus, the trends observed by Özdemir and Whitelaw (1992) are repeated here. Thus, the present analysis, gives us a strong hint that a possible linear behavior of *A* as a function of the maximum jet velocity would be in order.

Despite our brief account of the problem of an orthogonal jet impinging on a wall, the following findings are remarkable: 1) the variations both *A* configurations is marked, 2) the level in the logarithmic expressions for the laws of the wall have a weak tendency to increased with increasing maximum jet velocity and wall temperature.

Thus, it appears that the trends observed by Özdemir and Whitelaw (1992) for the behavior of the velocity law of the wall is also followed by the temperature law of the wall.

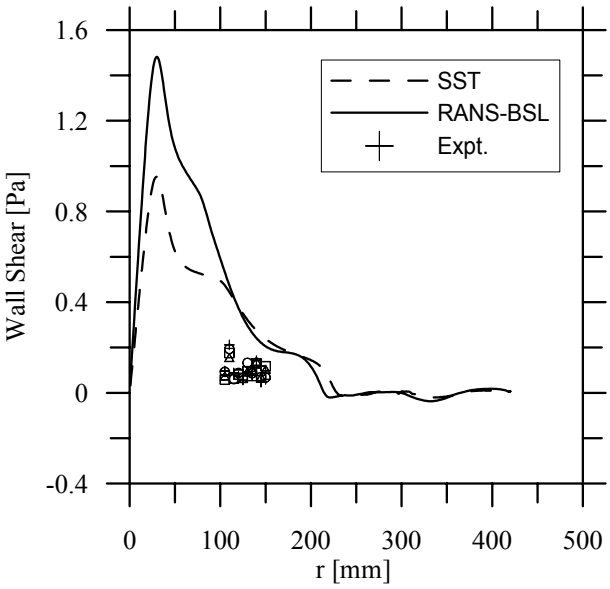

Figure 8. Deviation function for the velocity and the temperature profiles.

6. Conclusion

The present work has described the behavior of a semi-confined impinging jet over a flat plate. Experimental data for the pressure distribution, the mean and fluctuating velocities were obtained. The existence of a velocity equilibrium layer was also investigated. The results found at this preliminary investigation indicate that the level of the logarithmic portion of the velocity law of the wall increases with increasing maximum jet velocity.

The present research is particularly relevant because, in their research, Wygnanski et al. (1992) have decided that the most reliable method for measuring the wall stress is to use the slope of the mean velocity profile near the surface. This method was tested against floating drag balances, Preston tubes and the momentum integral equation.

Acknowledgements. APSF is grateful to the Brazilian National Research Council (CNPq) for the award of a research fellowship (Grant No 304919/2003-9). The work was financially supported by CNPq through Grant No 472215/2003-5 and by the Rio de Janeiro Research Foundation (FAPERJ) through Grants E-26/171.198/2003 and E-26/152.368/2002. BRSG is grateful to the CNPq for the award of a scholarship.

7. References

Behnia, M., Parneix, S. and Durbin, P. A., 1998, "Prediction of heat transfer in an axisymmetric turbulent jet impinging on a flat plate", Int. J. Heat and Mass Transfer", Vol. 41, No. 12, pp. 1845-1855.

Behnia, M., Parneix, S., Shabany, Y. and Durbin, P. A., 1999, "Numerical study of turbulent heat transfer in confined and unconfined impinging jets", Int. J. Heat and Fluid Flow, Vol. 20, pp. 1-9.

Craft, T. J., Graham, L. J. W. and Launder, B. E., 1993, "Impinging jet studies for turbulence model assessment-II. An examination of the performance of four turbulence models", Int. J. Heat Mass Transfer, Vol. 36, No. 10, pp. 2685-2697.

Coles, D., 1956, "The law of the wake in a turbulent flow", J.F.M., Vol. 1, pp. 191.

Cruz D. O. A. and Silva Freire A. P., 1998, "On single limits and the asymptotic behavior of separating turbulent boundary layers", Inter. J. Heat and Mass Transfer, Vol. 41, pp. 2097-2111.

Gibson, M. M. and Harper, R. D., 1997, "Calculation of impinging-jet heat transfer with the low-Reynolds-number q-ζ turbulence model", Int. J. Heat and Fluid Flow, Vol. 18, pp. 80-87.

Guerra, D. R. S. and Silva Freire, A. P., 2003, "An experimental heat transfer study of a cold jet impinging onto a hot surface", Congresso Brasileiro de Engenharia Mecânica, São Paulo, December.

Guerra, D. R. S. and Silva Freire, A. P., 2004, "A study of the heat transfer behaviour for a cold jet impinging upon a hot surface", Congresso Nacional de Engenharia Mecânica, Belém, August.

Guerra, D.R.S, Su, J. and Silva Freire, A. P., 2005, The near wall behavior of an impinging jet, International J. Heat and Mass Transfer.

Irwin, H. P. A. H., 1973, "Measurements in a self-preserving plana wall jet in a positive pressure gradient", J.F.M., Vol. 61, pp. 33.

Kendoush, A. A., 1998, "Theory of stagnation region heat and mass transfer to fluid jets impinging normally on solid surfaces", Chem. Eng. Processing, Vol. 37, pp. 223-228.

Kline, S. J.; 1985, The Purpose of Uncertainty Analysis, J. Fluids Engineering, 107, 153-160.

Lee, J. and Lee, S. -J., 1999, “Stagnation region heat transfer of a turbulent axisymmetric jet impingement”, Exp. Heat Transfer, Vol. 12, pp. 137-156.
Lee, J. and Lee, S. -J., 2000, “The effect of nozzle aspect ratio on stagnation region heat transfer characteristics of elliptic impinging jet”, Int. J. Heat Mass Transfer, Vol. 43, pp. 555-575.
Nishino, K., Samada, M., Kasuya, K. and Torii, K., 1996, “Turbulence statistics in the stagnation region of an axisymmetric impinging jet flow”, Int. J. Heat and Fluid Flow, Vol. 17, 193-201.
Ozdemir, I. B. and Whitelaw, J. H., 1992, “Impingement of an axisymmetric jet on unheated and heated flat plates”, J. Fluid Mech., Vol. 240, pp. 503-532.
Sigalla, A., 1958, “Measurements of a skin-friction in a plane turbulent wall jet”, J. R. Aero. Soc., Vol. 62, pp. 873.
Shu, J.-J. and Wilks, G., 1996, “Heat transfer in the flow of a cold, two-dimensional vertical liquid jet against a hot, horizontal plate”, Int. J. Heat Mass Transfer, Vol. 37, No. 16, pp. 3367-3379.
Wygnanski, I., Katz, Y. and Horev, 1992, “On the applicability of various scaling laws to the turbulent wall jet, J.F.M., Vol. 234, pp. 669-690.